2689

p17

NASA Technical Memorandum 103779

Experimental Study of Boundary Layer Transition on a Heated Flat Plate

K.H. Sohn and E. Reshotko
Case Western Reserve University
Cleveland, Ohio

and

K.B.M.Q. Zaman
Lewis Research Center
Cleveland, Ohio

NASA
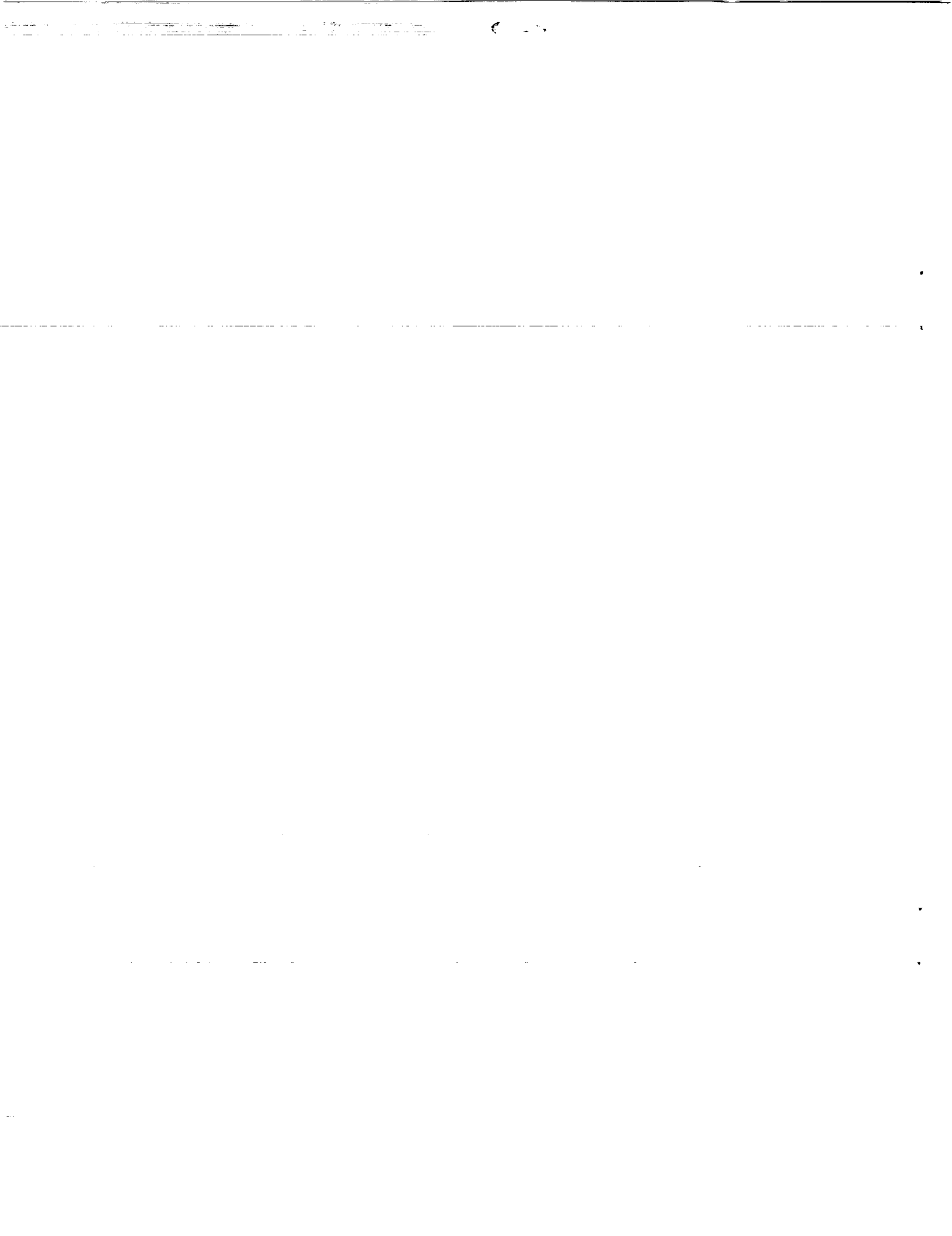
EXPERIMENTAL STUDY OF BOUNDARY LAYER TRANSITION ON A HEATED FLAT PLATE

K.H. Sohn and E. Reshotko
Department of Mechanical and Aerospace Engineering
Case Western Reserve University
Cleveland, Ohio 44106

and

K.B.M.Q. Zaman
National Aeronautics and Space Administration
Lewis Research Center
Cleveland, Ohio 44135

ABSTRACT

A detailed investigation to document momentum and thermal development of boundary layers undergoing natural transition on a heated flat plate was performed. Experimental results of both overall and conditionally sampled characteristics of laminar, transitional and low Reynolds number turbulent boundary layers are presented. Measurements were done in a low-speed, closed-loop wind tunnel with a freestream velocity of 100 ft/s and zero pressure gradient over a range of freestream turbulence intensities from 0.4 to 6 percent. The distributions of skin friction, heat transfer rate and Reynolds shear stress were all consistent with previously published data. Reynolds analogy factors for momentum thickness Reynolds number, $Re_\theta < 2300$ were found to be well predicted by laminar and turbulent correlations which accounted for an unheated starting length and uniform heat flux. A small dependence of turbulent results on the freestream turbulence intensity was observed.

INTRODUCTION

The understanding of boundary layer development under the influence of a highly disturbed freestream is important for many engineering applications. This is especially so for turbine blades of aircraft gas turbine engines. Heat transfer rates from hot gases to cooled turbine blades are largely dependent on whether the boundary layer is laminar, transitional or turbulent. Since boundary layer transition is characterized by a significant increase of skin friction and heat transfer rate, the determination of the transition location on the turbine blade becomes necessary to accurately predict local heat transfer rates and then to properly assess the cooling requirements for the turbine blade (Graham, 1979). On turbine blades, the transition process is extended over appreciable portions of the cooled surface. Heat transfer measurements by Turner (1971) indicated that transitional behavior was observed over about 80 percent of the suction side of a typical turbine blade for a freestream turbulence level of 5.9 percent. The accurate prediction of the transition pattern leads directly to

the improvement of engine efficiency and hardware durability. More reliable information from systematic and well-controlled experiments are required to provide fundamental information for improved modeling and computation of boundary layer transition as it occurs in turbomachinery. This is the motivation of the current work.

Previous studies of the influence of pressure gradient and heat transfer rate as well as freestream disturbances on boundary layer transition were primarily concerned with the mean overall characteristics of intermittent boundary layers. The effects of heat transfer in addition to freestream turbulence level and pressure gradient were considered experimentally by Junkhan and Serovy (1967) on a heated constant temperature wall, by Blair (1982) on a uniformly heated flat plate and by Rued and Wittig (1985) on a cooled isothermal wall. They observed that the effect of heat transfer on boundary layer transition is not significant compared to the corresponding effects of freestream turbulence and pressure gradient. Transition Reynolds number was relatively insensitive to wall heat transfer rate and mild acceleration of the flow. Gaugler (1985) has summarized a number of bypass transition data sets that include the effects of heat transfer, covering a wide range of flow conditions and indicating strong effects of freestream turbulence level and pressure gradient on the location and length of the transition zone. He concluded that the transition length appeared to depend strongly on the freestream parameters within the zone rather than just on the conditions at the start of transition. A general review of transition mechanisms (T-S and bypass modes) and of the prediction and control of transition was presented by Reshotko (1986).

Several other very recent studies of Blair (1988) for mildly accelerating flow, of Kuan and Wang (1988) and Kim, Simon and Kestoras (1989) for flat plate boundary layer flow focused additionally on determination of the separate statistics of the non-turbulent and turbulent parts of the transitional boundary layer using conditional sampling techniques. Results of these studies clearly indicated that the non-turbulent and turbulent parts in the transitional

flow cannot be thought of respectively as Blasius and fully turbulent flows.

The present experimental study was conducted on a uniformly heated flat plate with zero pressure gradient for freestream turbulence intensities ranging from 0.4 to 6 percent. The first part of this experimental program is to document the momentum and thermal mean characteristics of laminar, transitional and low Reynolds number turbulent boundary layers. In addition to mean and rms velocity and temperature profiles, the Reynolds analogy factors are determined for six levels of freestream turbulence. The second part examines correlations of instantaneous velocities and temperature measured simultaneously with a miniature 3-wire probe. Reynolds shear stress and turbulent heat flux are discussed.

EXPERIMENTAL FACILITY

The experiments were performed in a low-speed, closed-circuit wind tunnel located at the NASA Lewis Research Center. This wind tunnel was designed to generate large-scale, two-dimensional, incompressible boundary layers and to study the effects of freestream turbulence, pressure gradient and heat transfer rates on the transitional boundary layer. Upon exiting the blower, the air enters the flow-conditioning plenum chamber, where any flow irregularities introduced by the blower are removed and the freestream turbulence levels are reduced. At the downstream end of the flow-conditioning chamber and upstream of the contraction nozzle, turbulence generating grids could be positioned to set the freestream turbulence in the test section.

The test section of the wind tunnel is rectangular in cross section and measures 27 in. wide, 60 in. long and 6 in. high. At the entrance to the test section, a double bleed scoop assembly is positioned. The large scoop is intended to remove both the boundary layer which develops along the contraction nozzle and the vortices which develop in the contraction corners. The small scoop, smoothly attached to the test surface, serves as the leading edge of the flat plate, which is a 4:1 ellipse. This arrangement results in a 1.375-in. unheated starting length. This small scoop bleeds off any boundary layer which develops on the large scoop.

The heated flat plate model is constructed using 12-in. sections of rigid polyurethane foam, 27 in. wide, 2 in. thick, and totaling 56 in. in length. The inconel foil was cemented to the foam to form the test surface. The test surface is uniformly heated using nine strips of 6-in. wide, 24-in. long and 0.001-in. thick inconel foil. The area of the heated surface is 9 ft^2. The surface temperatures were measured by means of thermocouples spot-welded directly to the back side of the foil through small holes in the rigid foam plate. For more detailed experimental procedure, facility and instrumentation, refer to Sohn and Reshotko (1991).

Two types of probes were used in this experimental work: (1) A commercially available single sensor boundary layer hot-wire probe was used to measure the streamwise component of mean and fluctuating velocity. This probe was also operated in constant current mode to measure the mean temperature in the boundary layer. (2) A miniature 3-wire probe was used to simultaneously measure the instantaneous streamwise and vertical components of velocity and the temperature. This also allowed the determination of correlation quantities like Reynolds shear stress and turbulent heat flux in the boundary layer.

The 3-wire probe was designed based on the requirement of having good spatial resolution and the ability to make measurements as close to the wall as possible. The two velocity sensors have an X shape with ±45° orientation. These X sensors are 2.5 μm gold plated tungsten wires with a sensing length of 0.5 mm, which gives l_w/d_w = 200. To reduce the prong interference and end-wall conduction, the wires were plated. The overall length of each X-wire including the plated portions is 1 mm. The temperature sensor is an unplated 1 μm platinum wire with a length of 0.35 mm, yielding l_w/d_w = 350. These three wires are separated 0.35 mm apart from each other. Thus, the spanwise separation of the wires of the 3-wire probe, S^+, is about 50 wall units for the worst case of a fully turbulent boundary layer.

RESULTS

Detailed momentum and thermal boundary layer measurements have been performed on a heated flat plate with zero pressure gradient. The nominal values of the freestream turbulence intensity are 0.4 percent for grid 0, 0.8 percent for grid 0.5, 1.1 percent for grid 1, 2.4 percent for grid 2, 5 percent for grid 3 and 6 percent for grid 4. For grids 0, 0.5, 1, and 2, the turbulence levels are almost constant with streamwise distance, which means that the grid-generated freestream turbulence quickly becomes nearly homogeneous for the relatively moderate levels of freestream turbulence less than 2 percent. However, the freestream turbulence levels for grids 3 and 4 indicate a slow decay with distance downstream due to larger eddies generated by the coarser grids, which means that turbulent cascading is still in progress.

The mean velocity profiles acquired at streamwise locations between X = 5 and 20 in. from the leading edge of the heated flat plate for grid 1 were normalized with wall units, u^+ and y^+. As shown in Fig. 1, the mean velocity profiles are compared to three types of reference curves: (1) $u^+ = y^+$, (2) the Blasius solution with a measured Re_θ for a laminar boundary layer, and (3) the Musker (1979) continuous law-of-the-wall curve for a fully turbulent boundary layer. Excellent agreement of the two upstream profiles with the Blasius curve is observed in profiles taken between X = 5 and 7 in. Note that the data points near the wall ($y^+ < 10$) are tightly bounded by $u^+ = y^+$ and the Musker law-of-the-wall curves. Farther downstream, the data fell in the region between the Blasius curve and the Musker law-of-the-wall curve. The profiles span nearly the entire range from laminar to turbulent boundary layers. Once the mean velocity profile fell close to the Musker law-of-the-wall curve especially in the log-linear region, it can be said that this might be the location of the end of transition.

The values of u_τ required to construct these plots were obtained from the mean velocity profiles depending on the characteristics of the boundary layers. The laminar values of u_τ were obtained from a laminar theory. The fully turbulent values of u_τ were obtained using the Clauser fit technique, and for the transition cases u_τ was acquired from the momentum integral theory.

The profiles of boundary layer mean temperature plotted in wall units, T^+ versus y^+, corresponding to the mean velocity profiles of Fig. 1 with the same conditions, are shown in Fig. 2. Three types of reference curves are also plotted along with the experimental data in these figures. These are: (1) $T^+ = Pr \cdot y^+$, (2) the theoretical laminar temperature

2

profile obtained by solving the momentum and energy equations simultaneously with proper boundary conditions, including a correction for unheated starting length, and (3) the temperature law-of-the-wall curve for fully turbulent boundary layers suggested by Kays and Crawford (1980) with constant values of $Pr = 0.708$ and $Pr_t = 0.9$. Due to the finite unheated starting length of 1.375 in., the profiles of theoretical laminar temperature deviate from the $T^+ = Pr \cdot y^+$ curve for almost all y locations. However, the theoretical laminar curve gets closer to the $T^+ = Pr \cdot y^+$ curve as Re_θ increases. Note that the values of u_τ used to construct these temperature profiles are the same values used to plot the corresponding mean velocity profiles. Excellent agreement of the farthest upstream laminar profiles ($X = 5$, 7 in.) with the corresponding theoretical laminar curves is observed. One striking feature observed in the transitional boundary layer is that the velocity profiles slightly lag the respective temperature profiles. This velocity lag can be clearly observed by comparing the mean velocity profiles at $X = 15$ in. to the corresponding temperature profiles, where the temperature profiles are in close agreement with temperature law-of-the-wall curve but the velocity profiles are still developing in the transitional region. This velocity lag is also reflected in the higher values of Reynolds analogy factor than $Pr^{-2/3}$. This result is, however, opposite in trend to the observations of Wang et al. (1985) and Kim et al. (1989).

The variation of the experimentally determined skin friction coefficient, C_f, with Re_θ is presented in Fig. 3. Negligible effect of freestream turbulence on laminar C_f but increasing values of C_f with freestream turbulence in the turbulent region were observed. One more trend observed in these skin friction profiles is that the boundary layer transition occurs at increasingly lower values of Reynolds number as the freestream turbulence level increases. The values of C_f for laminar and turbulent boundary layers are so different that C_f can be used to determine the transition region. The transition region thus determined is in good agreement with the region obtained from the mean velocity profiles.

A plot of Reynolds analogy factor, $2 \cdot St/C_f$, obtained for the condition of uniform heat flux in the range of $Re_x < 10^6$ ($Re_\theta < 2300$) for the six levels of freestream turbulence is shown in Fig. 4. Recall that the Reynolds analogy factor in air for a flat plate with zero pressure gradient and a thermal boundary condition of constant wall temperature is well represented by $Pr^{-2/3}$ for both laminar and turbulent flows. However, the reference curves representing the expected $2 \cdot St/C_f$ for laminar and turbulent regimes, are quite different from a conventional $Pr^{-2/3}$ curve due to the effects of the thermal boundary condition of uniform wall heat flux and an unheated starting length. Appropriate laminar and turbulent theoretical results suggested by Kays and Crawford (1980) were combined in order to obtain the curves shown. The value 0.332 comes from the laminar skin friction relation with constant fluid properties and 0.453 is from the laminar heat transfer relation with a uniform wall heat flux condition, resulting in a ratio of 1.365. The laminar values of $2 \cdot St/C_f$ is augmented by 36.5 percent solely due to the uniform wall heat flux condition over the constant wall temperature case, which indicates that the heat transfer rate is very sensitive to the thermal boundary condition in the laminar region. The term in the bracket accounts for the effect of unheated starting length which produces an additional augmentation of 17 percent at

the farthest upstream location ($X = 5$ in.) and diminishes to 5 percent at the far downstream measurement station ($X = 20$ in.). Consequently, values of $2 \cdot St/C_f$ as high as 2.0 can be expected in the laminar region. The turbulent correlation was treated quite similarly to the laminar correlation. For turbulent boundary layers, heat transfer results are much less sensitive to both thermal boundary condition (4.5 percent augmentation due to uniform heat flux) and unheated starting length (1 percent increase at $X = 20$ in.). Thus, the turbulent values are much closer to the well known $Pr^{-2/3}$ value of 1.26 with $Pr = 0.708$.

The experimentally determined laminar data agree very well with the laminar prediction. Examination of Fig. 4 reveals that the effect of freestream turbulence on $2 \cdot St/C_f$ in the laminar region is negligible. A progressive decrease of $2 \cdot St/C_f$ with increase of freestream turbulence level is also observed in the transition region. As known from the variation of skin friction and heat transfer, both C_f and St increase with increasing level of freestream turbulence in the transition region. The decreasing value of $2 \cdot St/C_f$ with increasing level of freestream turbulence in the transition region can be thus interpreted as a larger increase in C_f than in St. The values of $2 \cdot St/C_f$ for higher freestream turbulence cases (grids 3 and 4) in the post-transitional region are better predicted by $Pr^{-2/3}$ than by the turbulent correlation. The data for lower freestream turbulence cases (grids 0.5, 1 and 2), on the other hand, are closer to the values obtained from the turbulent correlation than $Pr^{-2/3}$. A slight increase of $2 \cdot St/C_f$ with freestream turbulence level in the turbulent region can also be detected.

The streamwise rms velocity fluctuations, u', within the boundary layer were measured at the same time as the mean velocity data were acquired. The profiles of the overall streamwise velocity fluctuations normalized with respect to U_e (streamwise component of turbulence intensities) across the boundary layer are presented in Fig. 5. Recall that the corresponding mean velocity profiles were presented in Fig. 1. The boundary layer profiles at $X = 5$ and 7 in. are believed to be laminar in the presence of freestream turbulence (pseudo-laminar boundary layer) with a peak value of rms u' occurring at $y/\delta^* \approx 1.3$, which is quite typical for the laminar boundary layer (Suder et al., 1988; Sohn and Reshotko, 1986; Wang et al., 1985).

The peak value of u'/U_e within the boundary layer grows rapidly and the peak moves toward the wall as the flow develops downstream in the transition region. The magnitude of near-wall peak is largest in the transition region. The maximum peak value of $u'/U_e \approx 0.13$ occurs at $y/\delta^* \approx 0.5$ in the early stages of transition as shown in the profile at $X = 11$ in.. As the transition proceeds, another peak begins to appear at $y/\delta^* \approx 2$. While the near-wall peak diminishes, the second peak grows for a while and then decreases before both peaks reach some constant plateau value of $u'/U_e \approx 0.075$ in the immature stage of the turbulent boundary layer. The double peak in the transitional boundary layer is typical and has been reported by many other researchers (Arnal et al., 1978; Suder et al., 1988; Kuan and Wang, 1988; Kim et al., 1989). This double peak in the overall rms velocity profiles is believed to be due to the velocity jumping quickly between laminar and turbulent levels in the passage of turbulent spots, introducing some artificial overall rms velocity values at that specific location. This kind of velocity behavior can be seen from the direct hot-wire signals measured at

3

near-wall locations. The velocity waveforms at near-wall locations ($y/\delta^* < 0.6$) are characterized by large positive excursions during the passage of turbulent spots so correspondingly large apparent overall rms values are observed, resulting in the near-wall peak of overall rms profiles. Similarly, negative velocity excursions occur during the passage of a turbulent spot, which results in a large rms contribution to the second hump in the overall profiles at vertical measurement stations located farther out in the boundary layer ($1.5 < y/\delta^* < 4$). See the overall rms profiles at X = 13 and 15 in.

The intermittent signals from the hot-wire probe were sampled continuously with the high speed A/D data converter. The conditional sampling technique was employed to distinguish the digitally recorded signals into turbulent-like and laminar-like sections. The method for making turbulent/non-turbulent decisions from the intermittent velocity signals was explained in detail in Sohn and Reshotko (1991).

The profiles of intermittency factor $\Gamma(y)$ across the boundary layer at some streamwise locations for grid 1 are shown in Fig. 6. In these figures the solid curve represents an error function distribution of intermittency factor which is a Gaussian integral curve, for the fully turbulent boundary layer as suggested by Klebanoff (1955). As shown in this figure, the intermittency profiles in the transition region do not decrease monotonically across the boundary layer. Instead, a peak is observed near the wall ($y/\delta^* \approx 1$) at relatively low intermittencies ($\Gamma < 0.8$). It can be suspected that the most frequent turbulent activity in the transitional boundary layer is taking place at one displacement thickness away from the wall in the early stages of transition. This near-wall drop-off of Γ is in good agreement with a vertical cross-sectional shape of turbulent spots which exhibits the leading and trailing edge overhangs as observed by Cantwell et al. (1978) and is also consistent with a recent result obtained by Kuan and Wang (1988). The decay of Γ toward zero in the outer region is possibly due to the entrainment of the freestream flow into the boundary layer and the peaked-top shape of turbulent spots, i.e. the flow passes the turbulent spots less frequently in the region of $y/\delta^* > 4$.

Plots of conditionally sampled mean velocity profiles normalized with wall units, obtained at the same streamwise locations as the intermittency profiles are shown in Fig. 7. Three profiles: non-turbulent, overall and turbulent parts of intermittent flow are shown in each of these figures along with the Blasius, $u^+ = y^+$ and the Musker curves for reference. The non-turbulent profiles represent the average of velocity data obtained during time segments when the indicator function was zero. The turbulent parts were obtained from the average of instantaneous velocities acquired during time segments when the indicator function was equal to one. The overall profiles were determined from a direct long time average of the digitally recorded data which include both non-turbulent and turbulent parts. Note that the Re_θ used for the Blasius profile was the result from the non-turbulent mean velocity profiles, not from the overall profiles.

Low-intermittency non-turbulent profiles at X = 9 in. agree well with the corresponding Blasius profiles. However, the non-turbulent profiles increasingly deviate from Blasius curves as the intermittency increases. The turbulent profile has its maximum deviation from the log-linear profile early in the transition process, having the appearance of low Reynolds number turbulent boundary layers with a large

wake region. As the transition proceeds, the deviation from the log-linear region in the turbulent profiles is diminished. When $\Gamma \approx 0.99$, the shape of turbulent profiles looks quite like that of fully turbulent boundary layer.

The distribution of conditionally sampled C_f is shown in Fig. 8. At the beginning of transition, the non-turbulent profile had a Blasius shape but the turbulent parts had quite different shapes from the fully turbulent boundary layer. As Γ increased, the non-turbulent parts were observed to deviate increasingly from the corresponding Blasius shapes, while the turbulent parts were observed to approach the shape of fully turbulent profiles. The conditionally sampled mean velocity and C_f results clearly indicate that the non-turbulent and turbulent flows during the transition cannot be treated simply as Blasius and fully turbulent flows, respectively. More detailed explanation of conditionally sampled profiles can be found in Sohn and Reshotko (1991).

One of main objectives of this experimental study is to provide a momentum and thermal data base for transitional and low Reynolds number turbulent boundary layer ($Re_\theta < 2300$) especially in a highly disturbed environment. In order to capture the high-frequency components of fluctuating velocity and temperature as well as their correlations through transition, simultaneous measurements in nonisothermal flow with a miniature 3-wire probe were made. With this 3-wire probe, the distributions of cross-stream velocity and temperature fluctuations, Reynolds shear stress as well as turbulent heat flux in a transitional boundary layer for a freestream turbulence intensity of 1.1 percent (grid 1) were obtained.

One of the profiles of streamwise rms velocity fluctuations measured at X = 13 in. for grid 1 with both the single and the 3-wire probe is presented in Fig. 9. Due to the vertical X-shape of the 3-wire probe, the near-wall peak of streamwise turbulence intensity obtained by the single-wire was not captured with the 3-wire probe. However, the location and magnitude of the second peak of u'/U_e as observed by both probes are in agreement within 5 percent each other.

The distribution of normalized vertical component of rms velocity with streamwise distance is shown in Fig. 10. The magnitude of rms v' is measured to be much smaller than the corresponding values of rms u' near the wall ($y/\delta^* < 2$). However, the two values are getting closer to each other in the outer region ($y/\delta^* > 5$) and finally are nearly identical outside the boundary layers. The evolution of the rms v' profiles is quite different from the corresponding rms u' profiles in the transitional region. Recall that the u'/U_e value of the near-wall peak increased suddenly to a maximum at X = 11 in. and then gradually decreased to the magnitude for the fully turbulent boundary layer in the latter stages of transition with distance downstream as shown in Fig. 5. However, the peak magnitude of v' is observed to increase gradually from $v'/U_e \approx 0.045$ at X = 9 in. to $v'/U_e \approx 0.07$ at X = 15 in., but nearly maintains that maximum value of $v'/U_e \approx 0.07$, thereafter. This is quite consistent with the result of Kuan and Wang (1988) in terms of magnitude and trend. In addition, the similarity of v' in the outer portion of the boundary layer ($y/\delta^* > 2$) in the latter stages of transition, which was also seen in the profiles of u', is observed. The evolution of u' and v' with distance downstream in the transitional boundary layer can be viewed as the redistribution of turbulent kinetic

energy in the steady shear flow (Tennekes and Lumley, 1972).

The development of Reynolds shear stress, $\overline{-u'v'}$ in the transitional boundary layer for a freestream turbulence intensity of 1.1 percent was computed from digitally recorded instantaneous signals in a post-processing data reduction. Figure 11 shows the distribution of correlation coefficient of u' and v' within the boundary layer. These profiles represent Reynolds shear stress normalized with the product of rms velocity fluctuations. Note that the vertical distance from the wall was normalized with boundary layer thickness, δ (the y value when $U = 0.995\ U_e$). In the early stages of transition, the correlation coefficients have peak values of about 0.2 around $y/\delta_{0.995} \approx 0.65$ at $X = 9$ in. and of about 0.3 around $y/\delta_{0.995} \approx 0.45$ at $X = 11$ in. and then decrease to the freestream value as the profiles reach the edge of the boundary layer. The correlation coefficients in the outer portions of the boundary layer ($y/\delta_{0.995} > 0.7$) at two streamwise locations of $X = 9$ and 11 in. are rather scattered due to the very small rms values of u' and v'. It can be said that when the intermittency is less than some threshold value (about 0.5 in this study) the correlation coefficients are somewhat meaningless because the values of both numerator and denominator in the correlation coefficient are relatively small. However, with distance downstream, the correlation coefficient becomes larger and the locations of the constant plateau values of correlation coefficient move toward the wall. For profiles at $X = 20$ in. when the nominal intermittency factor is about 0.99 the plateau value of the correlation coefficient is 0.42 in the range of $0.1 < y/\delta_{0.995} < 0.4$ (this is somewhat less than the fully turbulent correlation coefficient). A correlation coefficient for a fully turbulent boundary layer of between 0.45 and 0.54 was reported by other researchers (Chen and Blackwelder, 1978; Senda et al., 1980; Blair, 1987).

One thing to be mentioned about the data measured with the 3-wire probe is that large effects of eddy averaging are possibly involved in the data obtained with the X-shaped sensing wires in the thin layer of shear flow at the early stages of transition ($l_w/\theta \approx 1.35$ at $X = 9$ in. and $l_w/\theta \approx 1.01$ at $X = 11$ in.; l_w is the hot-wire sensor length). Thus, in order to obtain more accurate data in a thin boundary layer without having significant averaging effects, the wire should be shorter which would require a very fine sub-micron diameter wire. This is not feasible, however. As transition proceeds, the boundary layer is getting thicker and the effect of l_w/θ is diminished ($l_w/\theta \approx 0.41$ at $X = 20$ in.). To confirm that the probe size effect in the thicker boundary layer is small, the $-u'v'$ profile was measured also at $X = 20$ in. for grid 3. The Reynolds shear stress profile for grid 3 agrees well with that of the fully turbulent boundary layer reported by others, having a near-wall peak value of $-u'v'/u_\tau^2$ of 1.0 and monotonically decreasing to zero in the freestream (Sohn and Reshotko, 1991). The Reynolds shear stress data obtained with the present probe configuration, thus, seem to be free from severe probe size effects.

In order to directly obtain the instantaneous temperature without solving a series of nonlinear heat transfer equations for a fine wire, the temperature sensor was operated with the constant current mode of the temperature bridge. However, due to the heat capacity of a temperature wire operated in a constant current mode, adequate frequency resolution for the temperature fluctuations was difficult to achieve with commercially available 5 μm diameter wire. Therefore,

a miniature 3-wire probe having a 1 μm diameter temperature wire was designed to properly achieve a good frequency response up to a few KHz. This frequency limit was considered adequate for the present experiment at low-speed, low-overheat flow with maximum temperature difference between wall and freestream of about 15 °F.

The distribution of fluctuating temperature normalized with ΔT ($= T_w - T_e$) within the transitional boundary layer for grid 1 is presented in Fig. 12. In the early stage of transition at $X = 9$ in., the rms t' profile merely shows the monotonic decrease from the value of 0.065 at $y/\delta^* \approx 1$ to the freestream uncertainty level. Due to the vertical X shape of the 3-wire probe, locating the temperature probe closer to the wall was not possible. No near-wall peak is thus observed at any streamwise station. As the intermittency increases, a peak which is probably the second peak, begins to appear at $y/\delta^* \approx 2$. The magnitude of the peak $t'/\Delta T$, which is about 0.085 at the relatively small flat portion around $y/\delta^* \approx 2$ at $X = 11$ in., significantly increases to the maximum value of 0.11 at $X = 13$ and 15 in. and then gradually decreases to the magnitude of 0.075 at $X = 20$ in. as Γ approaches unity. A double peak can also be seen in the profile measured at $X = 17.5$ in. In addition, the similarity of the rms temperature profiles in the outer portion ($y/\delta^* > 4$) of the boundary layer is also observed in the latter stages of transition. The trend, especially the vertical location and the maximum value of second hump in the rms temperature profiles is quite similar to that of the corresponding streamwise rms velocity profiles shown in Fig. 5. Therefore, as far as the rms values are concerned, the time-averaged data obtained with the miniature 3-wire probe are acceptable.

Turbulent heat flux, which is a correlation of fluctuating v' and t', was obtained from the digitally recorded instantaneous velocity and temperature signals. The distribution of turbulent heat flux normalized with the product of respective rms values (correlation coefficient) in the transitional boundary layer is shown in Fig. 13. The values of turbulent heat flux in the transitional boundary layer are found to be negative except in the region of $y/\delta_{0.995} > 0.4$ at $X = 20$ in.. The nominal intermittency factors corresponding to these data for grid 1, range from $\Gamma \approx 0.34$ to 0.99. The negative correlation indicates that v' and t' are out of phase in these flows. Since the mean temperature gradient is negative in the boundary layer, the negative correlation between v' and t' seemingly indicates that the average heat flux generated by the fluctuating flow is directed toward the wall. This is a peculiar result not reported in any previous studies.

The above behavior is observed principally in the transitional boundary layers. The values of the turbulent heat flux increase, however, as intermittency or Reynolds number increases and finally become positive at $y/\delta_{0.995} \approx 0.4$ when $\Gamma \approx 0.99$ and $Re_\theta \approx 1150$ ($X = 20$ in., G1). The value of the correlation coefficient of $\overline{v't'}$ over the most part of a fully turbulent boundary layer is measured to be 0.5 by other researchers (0.51 for Chen and Blackwelder (1978) at $Re_\theta \approx 2900$ and 0.55 for Blair (1988) at $Re_\theta \approx 5400$). Obviously, the presently measured small positive value of this quantity even when $\Gamma \approx 0.99$ contrasts with these earlier experimental results. To check if the correlation coefficient would approach 0.5 with increasing Re_θ, the flow was disturbed by the coarser grid 3 and measurements were performed at further downstream locations i.e. at $X = 20$, 38, and

45 in.. The correlation coefficients measured at
X = 20 in. ($Re_\theta \approx 2000$), X = 38 in. ($Re_\theta \approx 2800$) and
at X = 45 in. ($Re_\theta \approx 3200$) for grid 3 are also shown
in Fig. 13. The values of correlation coefficient
clearly increase as Re_θ increases. However, the
profile of the correlation coefficient even at
X = 45 in. exhibit values lower than 0.5 as measured
by others. The profile shows a constant plateau value
of about 0.4 in the region of $0.4 < y/\delta_{0.995} < 0.8$ and
small negative values very close to the wall ($y/\delta_{0.995}$
< 0.05). The repeatability of this peculiar behavior
of $\overline{v't'}$ has been checked additionally with an analog
correlator. The validity and consistency between the
digital and analog results are reported in Sohn and
Reshotko (1991).

Thus the operation of the 3-wire probe and the
data reduction schemes seem both to have been properly
performed, and so the focus must shift to the 3-wire
probe itself. Since the spanwise separation of the
velocity and temperature sensors in the present 3-wire
probe configuration is relatively large (S $\approx$ 0.52 mm),
it is speculated that the correlation of v' and t'
may be improper. For a fully turbulent boundary layer
measured at X = 20 in. with grid 3 ($U_e \approx$ 100 ft/s,
$u_\tau \approx$ 4.6 ft/s), the spanwise distance between these
sensors in wall units, S^+ is about 46. This value of
S^+ is larger than the criterion of 20 suggested by
Ligrani and Bradshaw (1987) for resolving proper fine-
scale turbulent fluctuations especially in the near-
wall region. With the same probe geometry, the only
way to reduce the value of S^+ is to lower the free-
stream speed, which in turn decreases the value of
u_τ. Another set of $\overline{v't'}$ data was obtained with a
reduced freestream speed of 45 ft/s at the same
streamwise location of X = 20 in. for grid 3, result-
ing in $S^+ \approx$ 22. The profiles of correlation
coefficient of v' and t' across the boundary layer
with the two different values of S^+ measured at
X = 20 in. for grid 3 are shown in Fig. 14. Notice-
able improvement of $\overline{v't'}$ with the smaller value of
S^+ is clearly observed in this figure, even though
the shape is different from that of previously
reported data for the fully turbulent boundary layer.
No distinct constant plateau value around 0.5 is seen
and there are still small portions of negative $\overline{v't'}$
very close to the wall.

Of all the possible reasons for the negative
correlation of turbulent heat flux in the boundary
layer, excessive spanwise separation of the wires of
the multiple-wire probe could well be the crucial
factor affecting a proper correlation of v' and t'.
To resolve this issue, additional carefully controlled
measurements with various values of S^+ as well as
using another specially well-designed 3-wire probe are
being planned in both transitional and fully turbulent
boundary layers.

CONCLUSIONS

A detailed investigation of momentum and thermal
boundary layer development focusing on the boundary
layer transition process in the presence of freestream
turbulence and surface heat transfer, was carried out
on a heated flat plate with zero pressure gradient as
part of an ongoing research program. For each level
of freestream turbulence, the time-averaged overall
quantities measured with a boundary-layer type single-
sensor probe and thermocouples were used to determine
the macroscopic momentum and thermal characteristics
of laminar, transitional and low Reynolds number
turbulent boundary layers. The instantaneous veloc-
ities and temperatures were measured simultaneously

with a miniature 3-wire probe to determine correlation
quantities in transitional boundary layers.

Increasing values of C_f with increasing levels
of freestream turbulence in the turbulent region were
observed, but the effect was negligible in the laminar
regions. The location of boundary layer transition
moved progressively upstream with increasing levels of
freestream turbulence. Measured Reynolds analogy
factors were found to be well predicted by combining
appropriate correlations for the thermal boundary
conditions of uniform heat flux and unheated starting
length for the respective laminar and turbulent
regimes. The Reynolds analogy factors were not sensi-
tive to either thermal boundary condition or unheated
starting length in the turbulent region. The boundary
layer transition was also observed as a rapid increase
of the near-wall peak of rms u' at $y/\delta^* \approx 0.5$ and
the occurrence of a second peak at $y/\delta^* \approx 2$ due to
the switching effect between laminar and turbulent
states. This observation is consistent with previous
studies. The cross-stream velocity fluctuation (v')
indicated that a large degree of anisotropy existed
within the transitional boundary layer although
isotropy was achieved near the edge of the boundary
layer.

The rms fluctuating temperature profiles meas-
ured with the 3-wire probe exhibited a similar
development as the streamwise rms velocity profiles in
transitional boundary layers in terms of magnitude and
peak location, showing, for example, double humps at
intermediate values of intermittency. The profiles of
turbulent heat flux, $\overline{v't'}$ acquired from the digitally
recorded instantaneous velocity and temperature
signals indicated negative values in certain cases,
especially in the intermittent region. Excessive
spanwise separation of the wires of the 3-wire probe
could well be the crucial factor affecting a proper
correlation of v' and t'. Significant changes in
$\overline{v't'}$ were obtained in tests where the freestream
velocity was reduced to 45 ft/s. At this reduced
speed (and therefore reduced dimensionless separation
in wall units) $\overline{v't'}$ were more positive and approached
the levels observed by others in turbulent boundary
layers.

REFERENCES

Arnal, D., Juillen, J.C. and Michel, R. (1978),
  "Experimental Analysis and Computation of the
  Onset and Development of the Boundary Layer
  Transition," NASA TM-75325.
Blair, M.F. (1982), "Influence of Free-Stream
  Turbulence on Boundary Layer Transition in
  Favorable Pressure Gradients," ASME J. Engr. for
  Power, Vol. 104, pp. 743-750.
Blair, M.F. and Bennett, J.C. (1987), "Hot-Wire
  Measurements of Velocity and Temperature Fluctua-
  tions in a Heated Turbulent Boundary Layer,"
  J. Physics Engr., Vol. 20, pp. 209-216.
Blair, M.F. (1988), "Bypass-Mode Boundary Layer
  Transition in Accelerating Flows," submitted to J.
  Fluid Mech., November.
Cantwell, B.J., Coles, D. and Dimotakis, P.E. (1978),
  "Structure and Entrainment in the Plane of Symmetry
  of a Turbulent Spot," J. Fluid Mech., Vol. 87,
  pp. 641-672.
Chen, C.H.P. and Blackwelder, R.F. (1978), "Large-
  Scale Motion in a Turbulent Boundary Layer: A Study
  Using Temperature Contamination," J. Fluid Mech.,
  Vol. 89, pp. 1-31.

Clauser, F.H. (1956), "The Turbulent Boundary Layer," *Advances in Applied Mechanics*, Vol. IV, Academic Press, New York, pp. 1-51.

Gaugler, R.E. (1985), "A Review and Analysis of Boundary Layer Transition Data for Turbine Application," *NASA* CP-2386, pp. 81-93.

Graham, R.W. (1979), "Fundamental Mechanisms that Influence the Estimate of Heat Transfer to Gas Turbine Blades," *NASA* TM-79128.

Junkhan, G.H. and Serovy, G.K. (1967), "Effect of Free-Stream Turbulence and Pressure Gradient on Flat Plate Boundary-Layer Velocity Profiles and on Heat Transfer," *ASME J. Heat Transfer*, Vol. 89, pp. 169-176.

Kays, W.M. and Crawford, M.E. (1980), **Convective Heat and Mass Transfer**, 2nd ed., McGraw-Hill, New York.

Kim, J., Simon, T.W. and Kestoras, M. (1989), "Fluid Mechanics and Heat Transfer Measurements in Transitional Boundary Layer Conditionally Sampled on Intermittency," *presented at the 1989 ASME National Heat Transfer Conference*, Philadelphia, PA.

Klebanoff, P.S. (1955), "Characteristics of Turbulence in a Boundary Layer with Zero Pressure Gradient," *NACA* Rep. No. 1247.

Kuan, C.L. and Wang, T. (1988), "Some Intermittent Behavior of Transitional Boundary Layer," *Submitted to Experimental Thermal and Fluid Science*.

Ligrani, P.M. and Bradshaw, P. (1987), "Spatial Resolution and Measurement of Turbulence in the Viscous Sublayer Using Subminiature Hot-Wire Probes," *Experiments in Fluids*, Vol. 5, pp. 407-417.

Musker, A.J. (1979), "Explicit Expression for the Smooth Wall Velocity Distribution in a Turbulent Boundary Layer," *AIAA Journal*, Vol. 17, No. 6, pp. 655-657.

Reshotko, E. (1986), "Stability and Transition, How Much Do We Know ?," *presented at the 10th U.S. National Congress of Applied Mechanics*, Austin, Texas.

Rued, K. and Wittig, S. (1985), "Free-Stream Turbulence and Pressure Gradient Effects on Heat Transfer and Boundary Layer Development on Highly Cooled Surfaces," *ASME J. Engr. for Gas Turbines and Power*, Vol. 107, pp. 54-59.

Senda, M., Suzuki, K. and Sato, T. (1980), "Turbulence Structure Related to the Heat Transfer in a Turbulent Boundary Layer with Injection," *Turbulent Shear Flows*, Vol. 2, Springer-Verlag, pp. 143-157.

Sohn, K.H. and Reshotko, E. (1986), "Transition in a Disturbed Environment," *Case Western Reserve University* Rep. FTAS/TR-87-189 (Also, M.S. Thesis of K.H. Sohn, C.W.R.U., 1986).

Sohn, K.H. and Reshotko, E. (1991), "Experimental Study of Boundary Layer Transition with Elevated Freestream Turbulence on a Heated Flat Plate," *NASA* CR-187068 (Also, Ph.D. Thesis of K.H. Sohn, C.W.R.U., 1991)

Suder, K.L., O'Brien, J.E. and Reshotko, E. (1988), "Experimental Study of Bypass Transition in a Boundary Layer," *NASA* TM-100913 (Also, M.S. Thesis of K.L. Suder, C.W.R.U., 1988).

Tennekes, H. and Lumley, J.L. (1972), **A First Course in Turbulence**, 2nd ed., MIT Press, Massachusetts.

Turner, A.B. (1971), "Local Heat Transfer Measurements on a Gas Turbine Blade," *J. Mech. Engr. Sci.*, Vol. 13, No. 1, pp. 1-12.

Wang, T., Simon, T.W. and Buddhavarapu, J. (1985), "Heat Transfer and Fluid Mechanics Measurements in Transitional Boundary Layer Flows," *NASA* CP-2386, pp. 69-79.
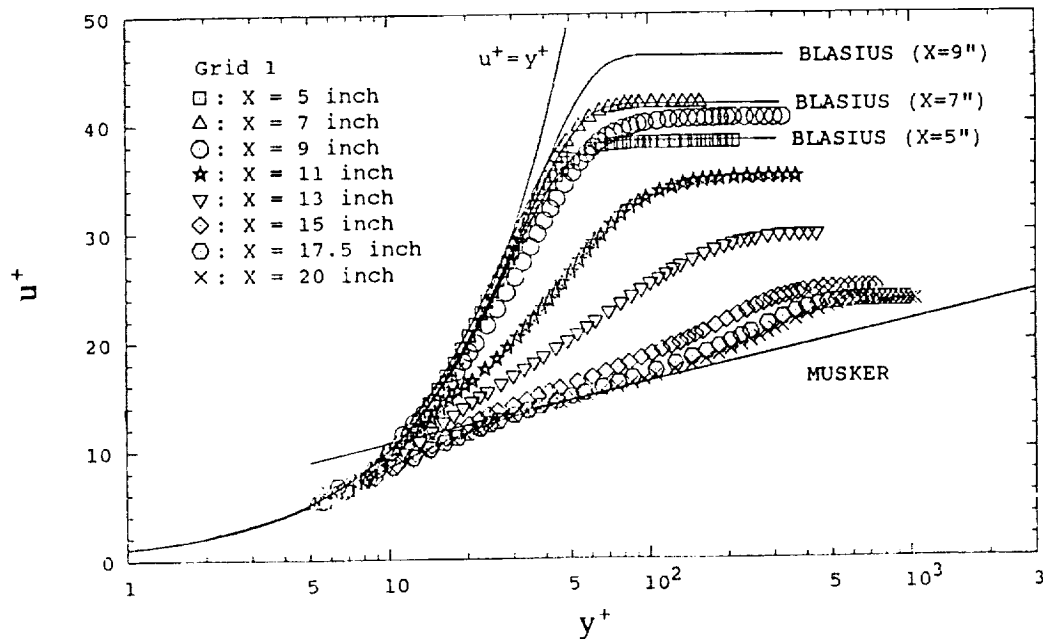
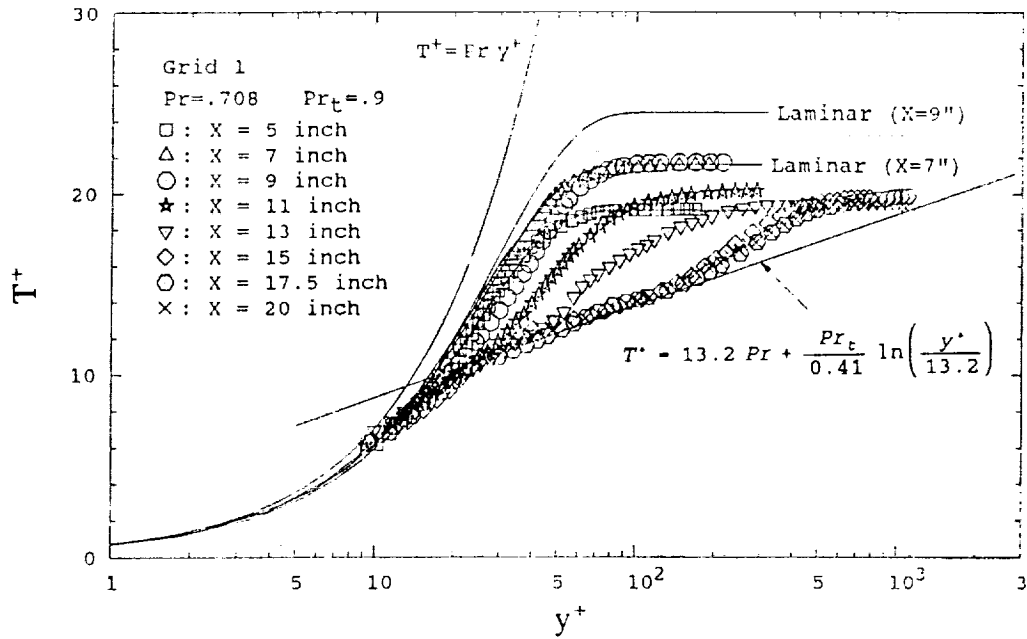Figure 1.—Streamwise mean velocity profile in wall units.
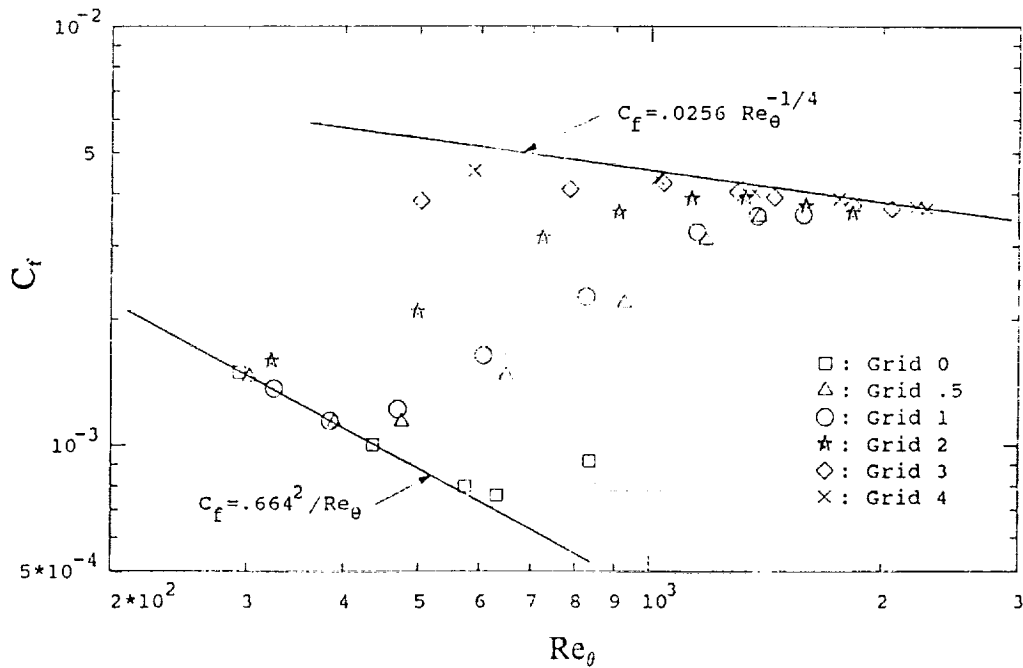
Figure 2.—Mean temperature profiles in wall units.

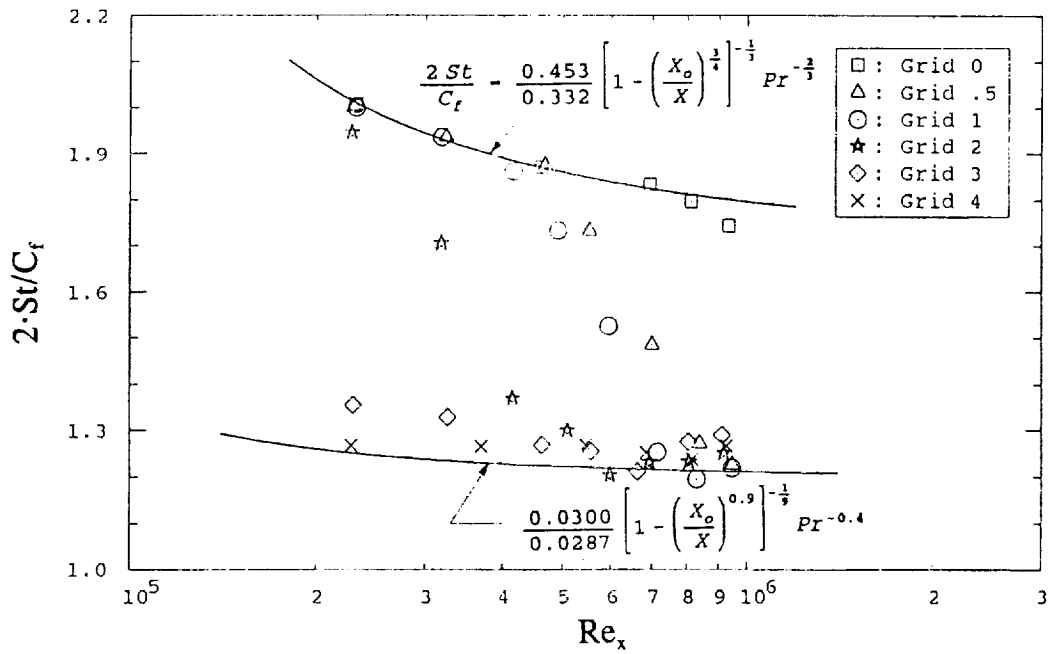Figure 3.—Skin friction coefficient dependence on Re_θ and freestream turbulence.

8

$$\frac{2\,St}{C_f} = \frac{0.453}{0.332}\left[1-\left(\frac{X_o}{X}\right)^{\frac{3}{4}}\right]^{-\frac{1}{3}} Pr^{-\frac{2}{3}}$$

□ :	Grid 0
△ :	Grid .5
○ :	Grid 1
★ :	Grid 2
◇ :	Grid 3
✕ :	Grid 4

$$\frac{0.0300}{0.0287}\left[1-\left(\frac{X_o}{X}\right)^{0.9}\right]^{-\frac{1}{9}} Pr^{-0.4}$$

$2 \cdot St/C_f$

Re_x

Figure 4.—Distribution of Reynolds analogy factor.

Grid 1

□ : X = 5 inch
△ : X = 7 inch
○ : X = 9 inch
★ : X = 11 inch
▽ : X = 13 inch
◇ : X = 15 inch
○ : X = 17.5 inch
✕ : X = 20 inch

u'/U_e

y/δ^*
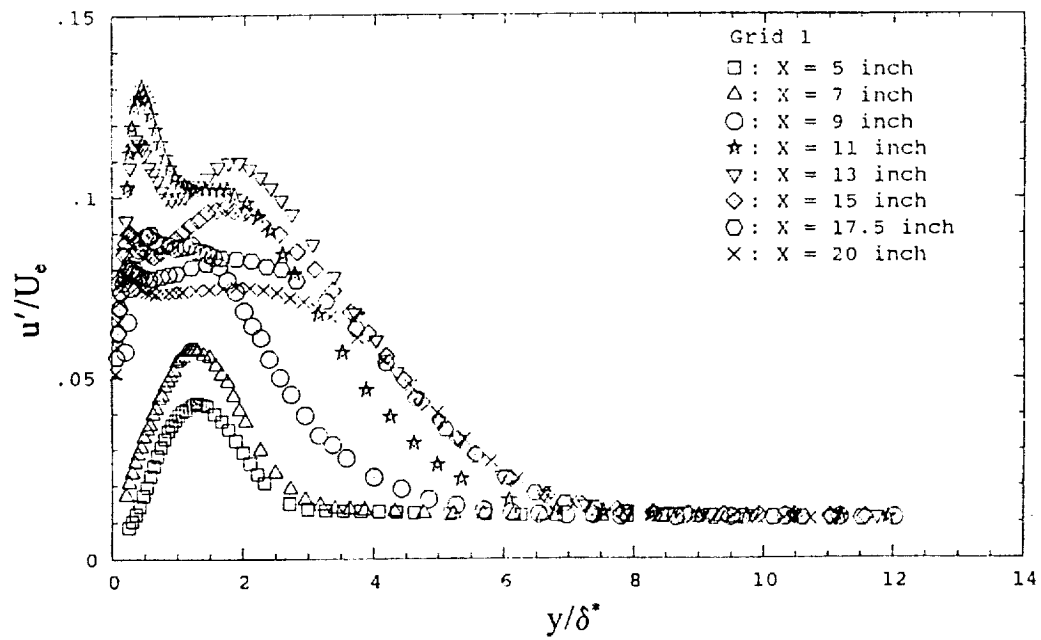
Figure 5.—Streamwise rms velocity profiles.

9
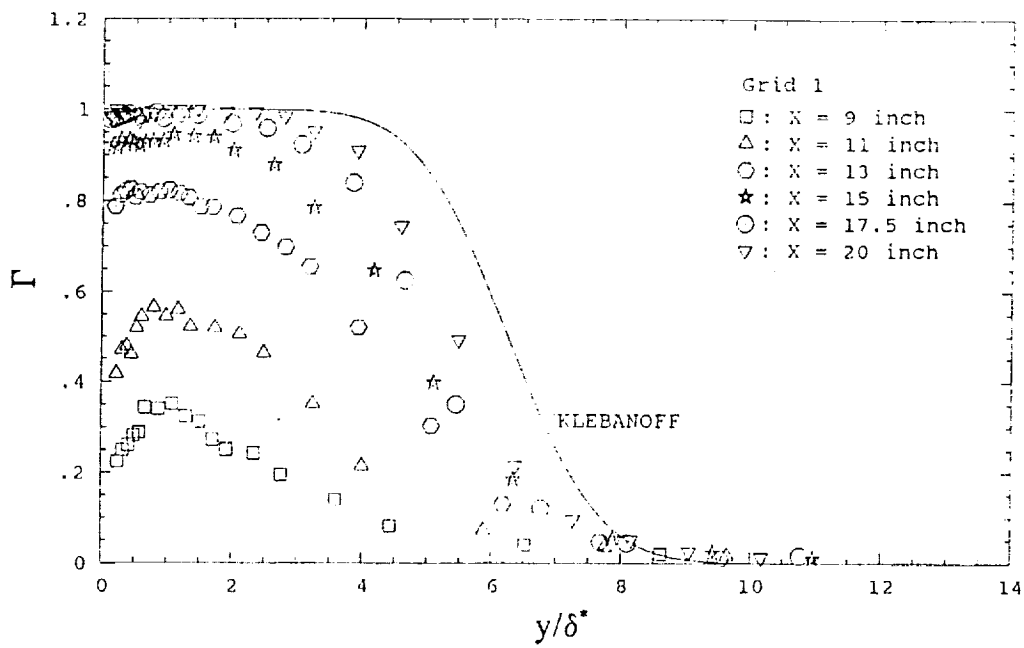
Figure 6.—Intermittency profiles across the boundary layer.
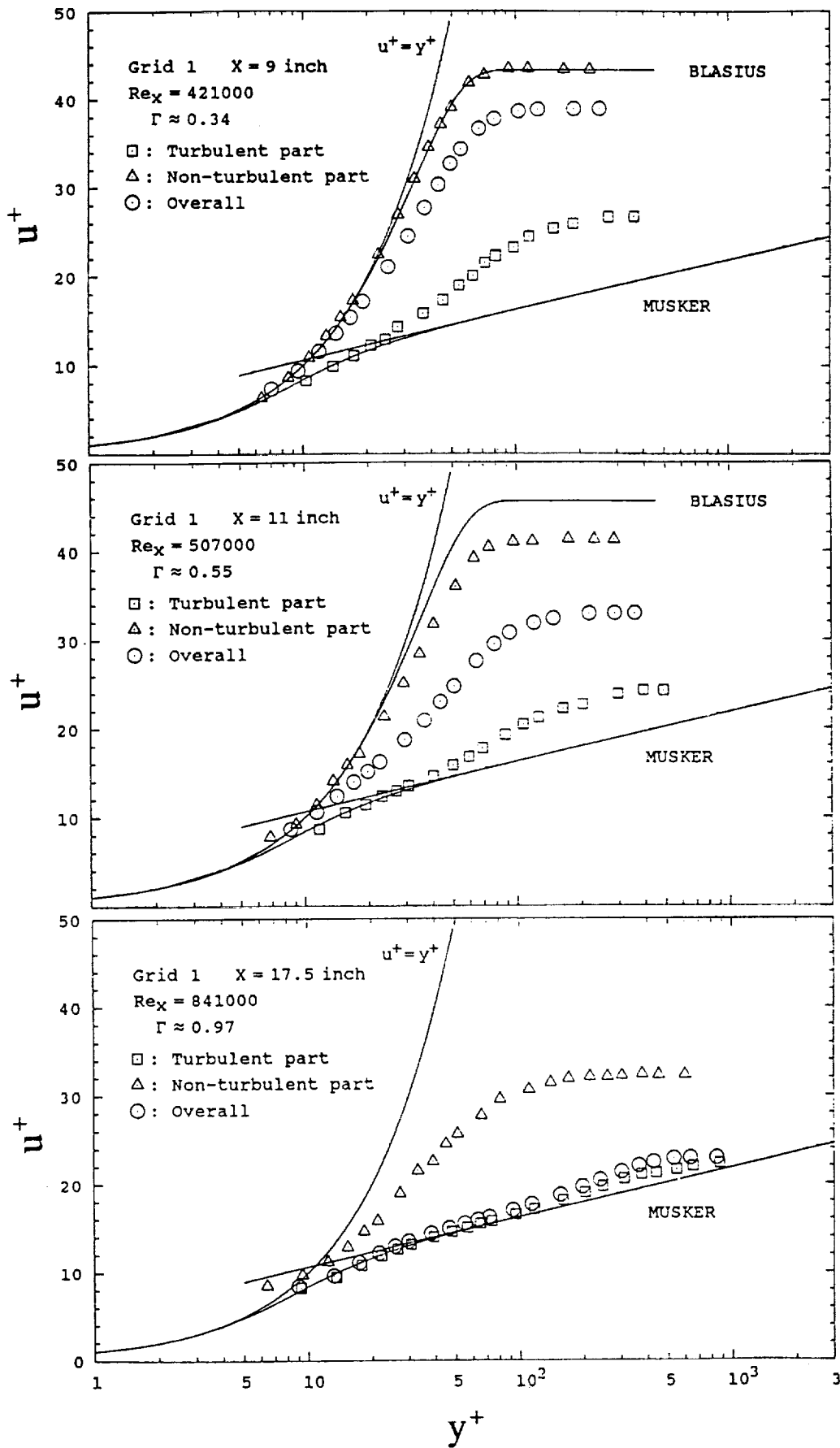
Figure 7.—Conditionally sampled mean velocity profiles in wall units.
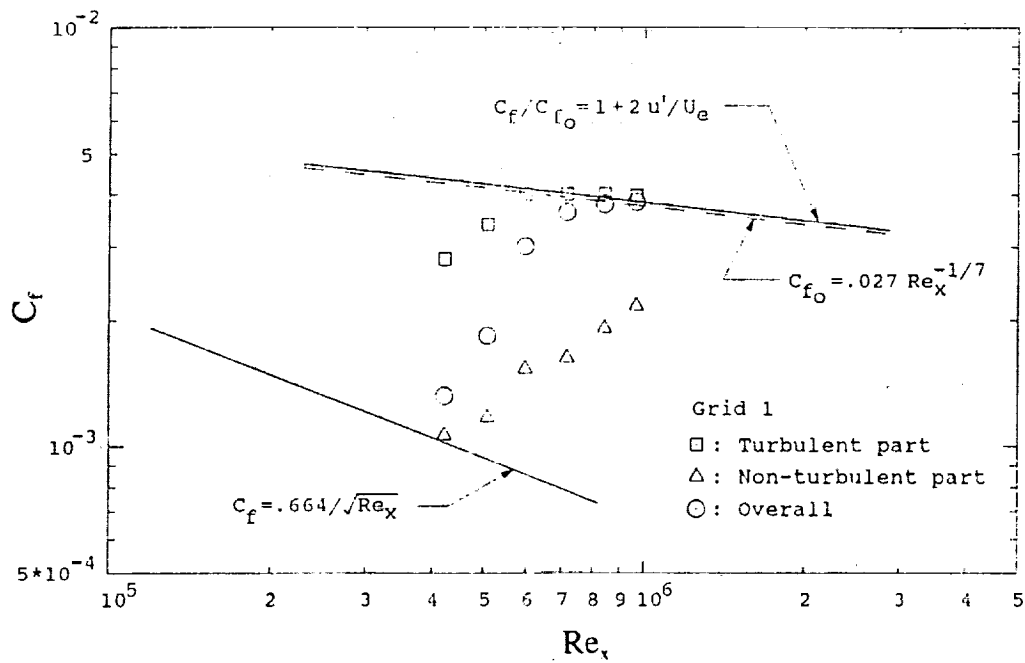
Figure 8.—Conditionally sampled skin friction coefficient profiles.
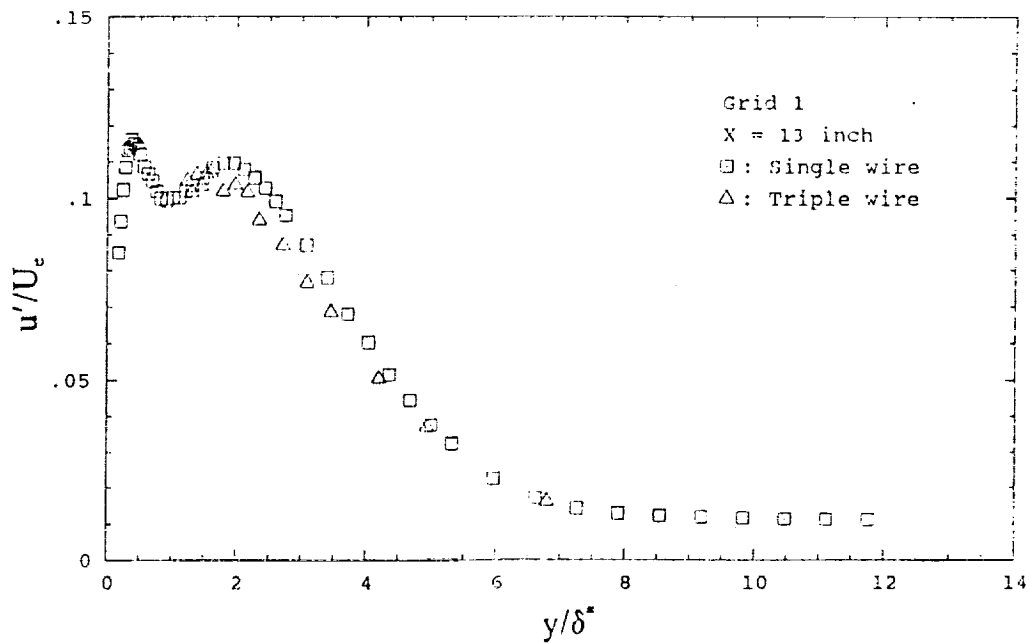
Figure 9.—Comparison of streamwise rms velocity profiles measured with single and 3-wire probes.

12
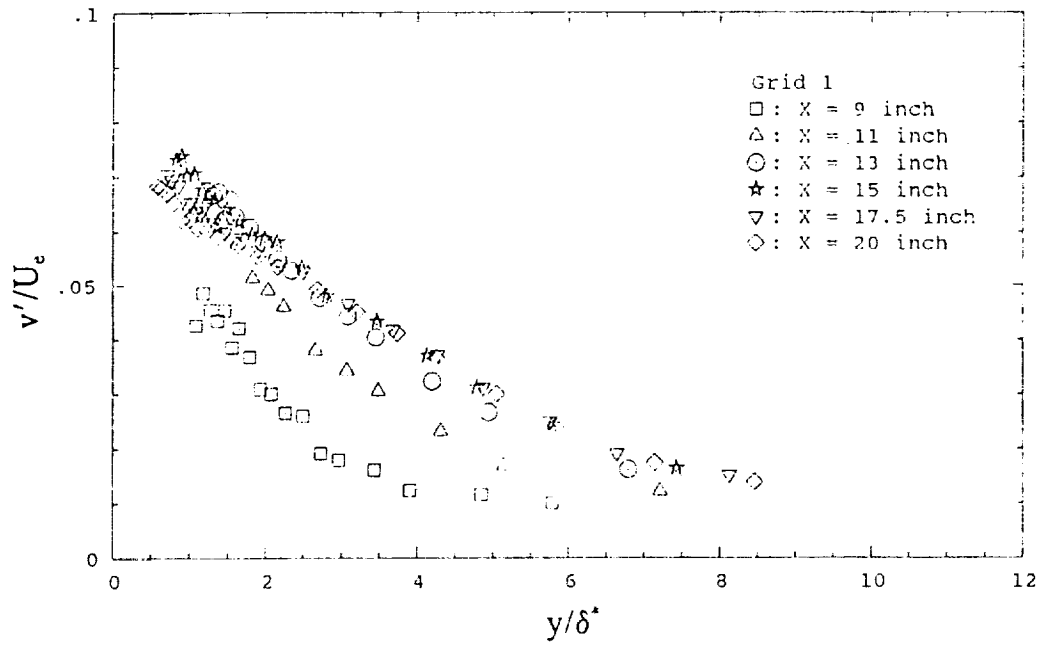
Figure 10.—Vertical component of rms velocity profiles.
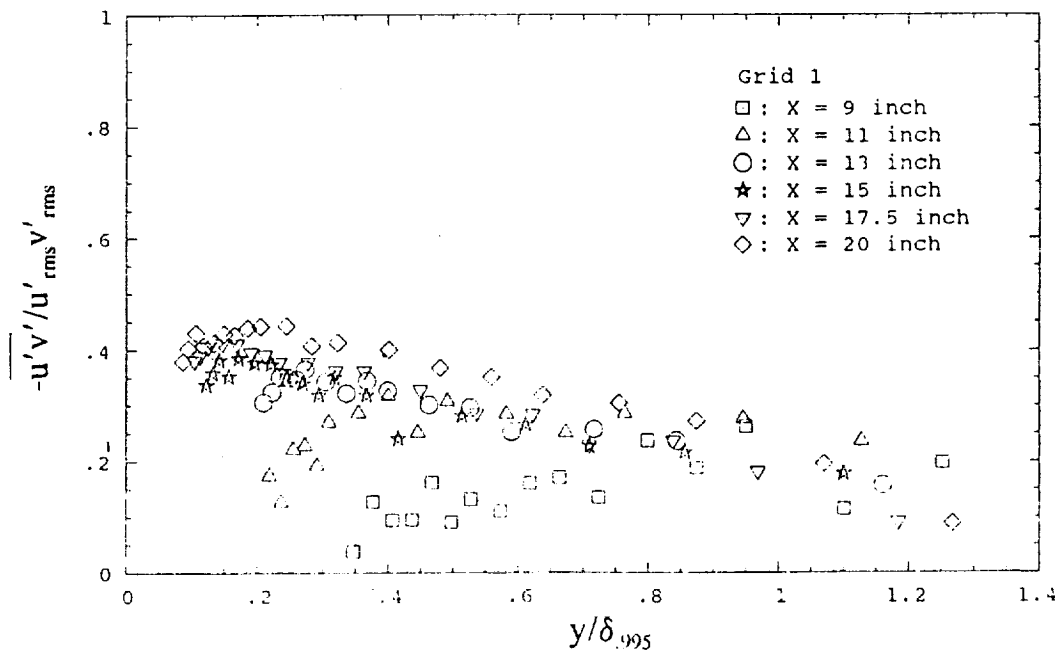
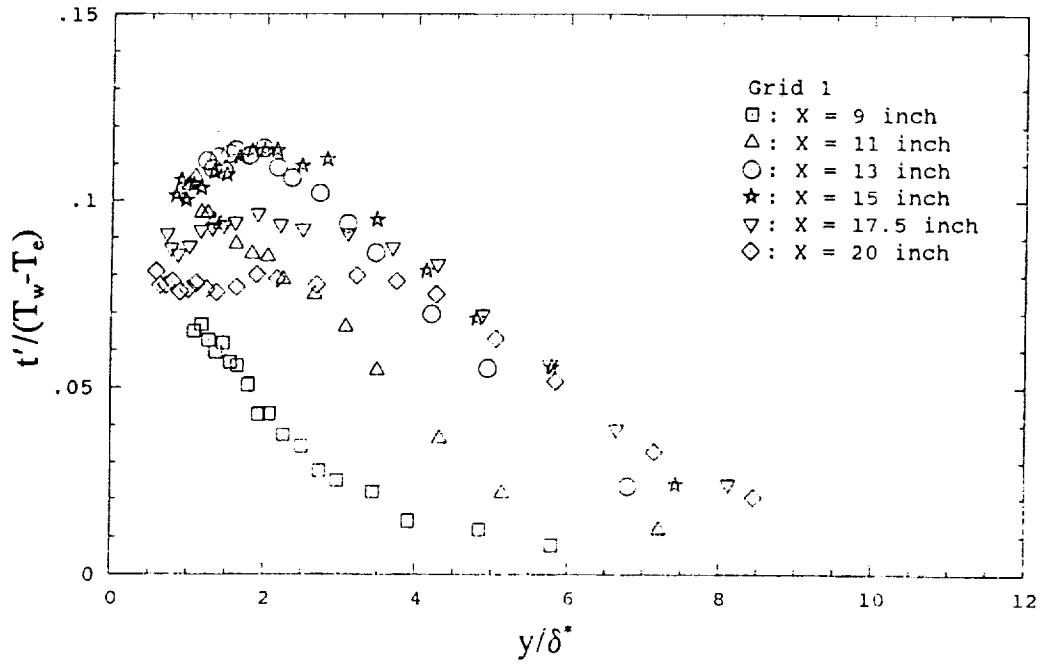Figure 11.—Correlation coefficient profiles of u' and v'.
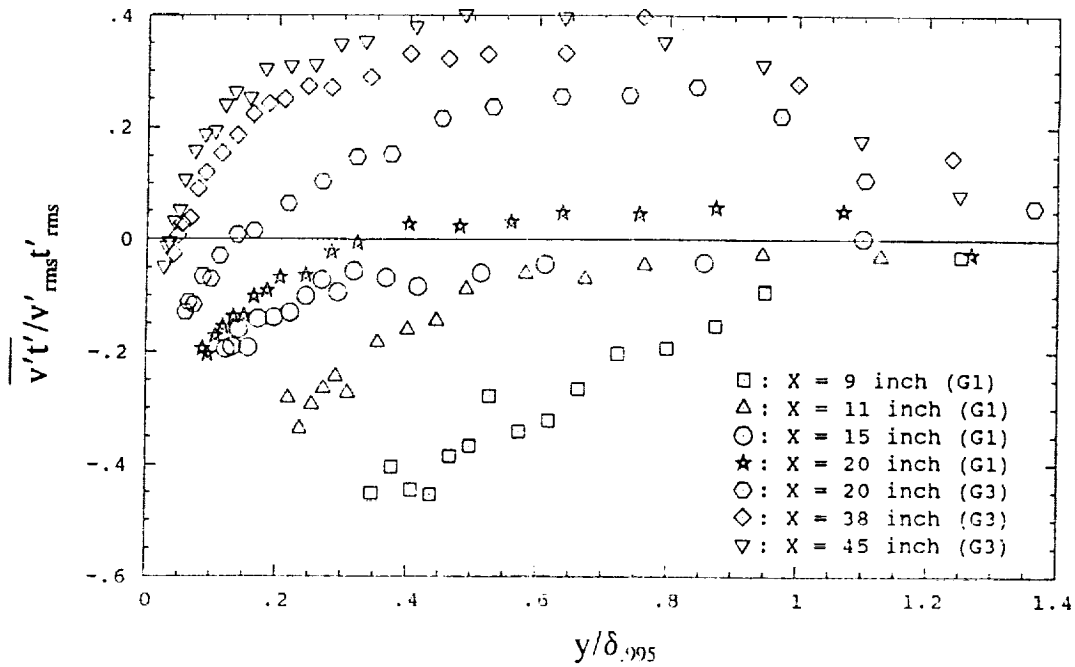
Figure 12.—RMS temperature fluctuation profiles.

Figure 13.—Correlation coefficient profiles of v' and t'.

14
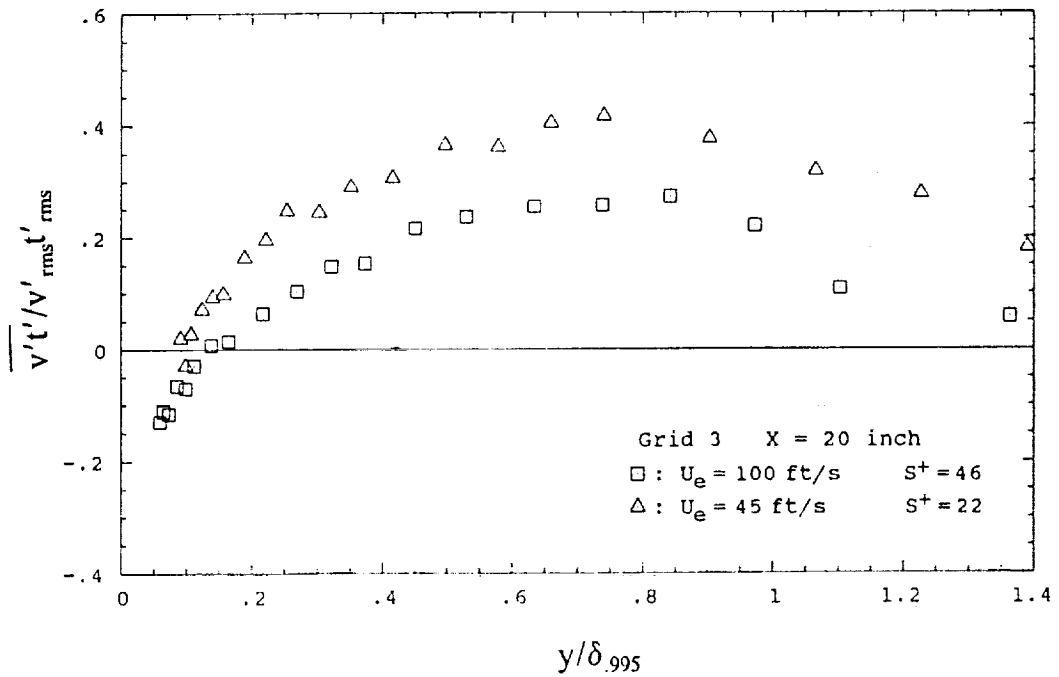
Figure 14.—Correlation coefficient profiles of v' and t' with different S^+.

NASA
National Aeronautics and Space Administration

Report Documentation Page

1. Report No. NASA TM - 103779	2. Government Accession No.	3. Recipient's Catalog No.

4. Title and Subtitle Experimental Study of Boundary Layer Transition on a Heated Flat Plate	5. Report Date
	6. Performing Organization Code

7. Author(s) K.H. Sohn, E. Reshotko, and K.B.M.Q. Zaman	8. Performing Organization Report No. E - 6050
	10. Work Unit No. 505 - 62 - 52

9. Performing Organization Name and Address National Aeronautics and Space Administration Lewis Research Center Cleveland, Ohio 44135 - 3191	11. Contract or Grant No.
	13. Type of Report and Period Covered Technical Memorandum

12. Sponsoring Agency Name and Address National Aeronautics and Space Administration Washington, D.C. 20546 - 0001	
	14. Sponsoring Agency Code

16. Abstract
A detailed investigation to document momentum and thermal development of boundary layers undergoing natural transition on a heated flat plate was performed. Experimental results of both overall and conditionally sampled characteristics of laminar, transitional and low Reynolds number turbulent with a freestream velocity of 100 ft/s and zero pressure gradient over a range of freestream turbulence intensities from 0.4 to 6 percent. The distributions of skin friction, heat transfer rate and Reynolds shear stress were all consistent with previously published data. Reynolds analogy factors for momentum thickness Reynolds number $Re_\theta < 2300$ were found to be well predicted by laminar and turbulent correlations which accounted for an unheated starting length and uniform heat flux. A small dependence of turbulent results on the freestream turbulence intensity was observed.

17. Key Words (Suggested by Author(s)) Tansition Heat transfer Boundary layer Flat plate	18. Distribution Statement Unclassified - Unlimited Subject Category 02

19. Security Classif. (of the report) Unclassified	20. Security Classif. (of this page) Unclassified	21. No. of pages 16	22. Price* A03